Semiconductor Physics, Quantum Electronics & Optoelectronics, 2008. V. 11, N 1. P. 54-58.

PACS 72.20.Dp, 72.20.-i, 81.10.Fq

Electrical properties of fast cooled InSe single crystals

A.V. Zaslonkin, Z.D. Kovalyuk, I.V. Mintyanskii, and P.I. Savitskii
I.M. Frantsevich Institute of Materials Science Problems,
National Academy of Sciences of Ukraine, Chernivtsi Department
5, Iryna Vilde str., 58001 Chernivtsi, Ukraine; e-mail: chimsp@ukrpost.ua

Abstract. Influence of fast cooling on electrical properties of *n*-InSe single crystals is investigated for an ingot grown by the Bridgman method. Electrical characteristics and their anisotropy are investigated in the temperature range 80 to 410 K. It is found that fast cooling, as soon as crystallization is completed, of the ingot leads to an increase of the free electron concentration, conductivity along layers, and conductivity anisotropy, as well as to a decrease of the Hall mobility of carriers along layers. The theoretical analysis of the mobility of carriers has shown that space-charge regions underlie the effective mechanism of their scattering.

Keywords: indium selenide, layered crystal, conductivity anisotropy, scattering mechanism.

Manuscript received 02.02.07; accepted for publication 07.02.08; published online 31.03.08.

1. Introduction

A crucial distinction between the chemical bonds along and across the layers in indium selenide determines the anisotropy of its physical properties and the peculiarities of applications in semiconductor electronics. Having the energy gap $E_g \sim 1.24$ eV and the free electron concentration $\sim 10^{15}$ cm^{-3} at the electron mobility $\sim 10^3$ cm^2/(V·s) at room temperature, the material is perspective for different semiconductor devices. In particular, InSe is a good candidate for photovoltaic conversion of the solar energy [1] as the inactivity of cleaved InSe surfaces to the adsorption of foreign impurities makes it possible to prepare efficient photosensitive barrier structures highly resistant to hard radiation by means of comparatively simple technologies [2]. The natural photopleochroism gives a possibility for creation of InSe-based polarized light analyzers [3]. An obvious potential of InSe is also related to its application as an intercalation cathode material in solid-state batteries [4], a host material for accumulation of hydrogen [5], and realization of its nano-structured forms.

However, the efficiency of the device structures is restricted to defects being appeared at the growing of single crystals. At the same time, it is known that, due to the peculiarities of the In – Se phase diagram [6] and the highest bond ionicity in indium monoselenide in comparison to other layered III-VI compounds [7], it is most difficult to obtain structurally perfect single crystals just of InSe. As electrical parameters and their dependence on different technological factors are concerned, they are at the first place in the fabrication of conventional semiconductor compounds. But the situation with InSe is exceptional to a considerable degree, and the disagreement between the literature data is high in comparison with other layered III-VI crystals. In particular, extremely different values of the conductivity components in the different crystallographic directions $\sigma_{\perp C}$ and $\sigma_{||C}$ (conductivities along and across the layers, respectively) have been observed in spite of the fact that the corresponding effective masses are related as $m^*_{\perp C} > m^*_{||C}$. This complicates the realization of potential advantages of InSe. For example, in InSe-based barrier structures, the series resistance increases, and the diffusion length of photocarriers become lower.

Therefore, technological experiments and investigations of different defects in InSe aimed at the fabrication of high-quality single crystals with stable and reproducible parameters keep their urgency. From the previous studies, it is known [8-10] that vacuum annealing of InSe single crystals affects their transport properties in different ways depending on the temperature, duration, and cooling conditions. In this paper, we first investigate the influence of fast cooling of an InSe ingot to room temperature as soon as the crystallization is completed. The electrical characteristics of the ingot are obtained, their anisotropy is measured, and the results are analyzed taking different scattering mechanisms into account.

© 2007, V. Lashkaryov Institute of Semiconductor Physics, National Academy of Sciences of Ukraine

2. Experimental

For investigations, an InSe single crystal was grown by the Bridgman method from a non-stoichiometric melt $In_{1.05}Se_{0.95}$. As usual, after a single crystal stops to grow, its cooling to room temperature takes place under conditions of a "switched-off" furnace (slow cooling) during 10 to 12 h. In our case, the cooling of the ingot of as-grown layered InSe has been carried out by means of the quick taking out of the ampoule from a heated furnace after the growth is completed. As a result, the cooling time was reduced to several tens of minutes. Since the ingot still remains in the field of a furnace temperature gradient after the growth termination, the samples for investigations were cut from its parts which had different temperatures before cooling: 450±5, 505±5, and 555±5 °C (samples 1 to 3, respectively).

The measurements of the Hall effect and conductivity along layers $\sigma_{\perp C}$ were performed with samples of rectangular form with typical dimensions of about 10×2×0.6 mm. Indium contacts to them were soldered in the classical configuration. The electron concentration n was determined from the Hall coefficient R_H using the relation $n = r / eR_H$ with the Hall factor $r = 1$. The measurements of the conductivity across layers $\sigma_{||C}$ were carried out on samples with typical dimension of the cleaved plane of about 4×5 mm and about 0.6 to 0.8 mm in thickness. Current contacts covered almost the whole cleaved surfaces, and the voltage was measured between a pair of small-area contacts close to them. Temperature dependences were measured in the range 80 to 400 K.

3. Results and discussion

The temperature dependences of the free electron concentration n are shown in Fig. 1 for fast cooled samples 1 to 3. The typical dependence for a slowly cooled InSe sample (curve 4) is also presented for comparison. The change of the electron concentration with temperature in the range $T < 300$ K is slight and practically the same for all the investigated crystals. But, in comparison with the slowly cooled crystals, the influence of fast cooling results in essentially higher values of n over all the temperature range. This indicates the presence of a shallow donor level in the energy gap of InSe which is already predominantly ionized at 77 K. It is generally accepted for this level to be related to interstitial In atoms [8, 9, 11, 12]. The activation energy of this level, established from electrical measurements [8, 9], is equal to 0.012–0.015 eV. At temperatures $T > 300$ K, the free electron concentration increases due to the ionization of a deeper donor level. Its activation energy ΔE, determined from the slope in the $\lg(nT^{-3/4}) = \varphi(10^3/T)$ dependence, is 0.38–0.40 eV. The presence of this level is not typical of slowly cooled InSe ingots with the same order of the free electron concentration.

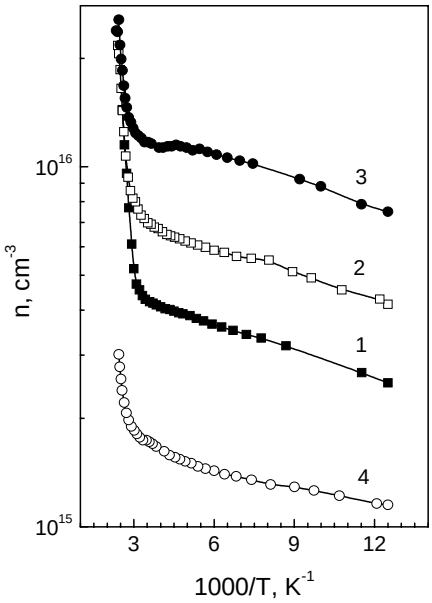

Fig. 1. Temperature dependences of the electron concentration for samples from the fast (1 to 3) and slowly (4) cooled InSe ingots. Curves 1 to 3 corresponds to the samples from the ingot parts with different temperatures before cooling: 450±5, 505±5, and 555±5 °C, respectively.

For all the investigated samples in the temperature range $T < 300$ K, the conductivity along the layers (Fig. 2) has "metallic" behavior. It takes place because the electron concentration increases more slightly with temperature in comparison with a decrease of the Hall mobility along the layers. Above room temperature, the conductivity has typical semiconductor character due to an abrupt increase of n. For the fast cooled samples, the $\sigma_{\perp C}$ values are essentially higher.

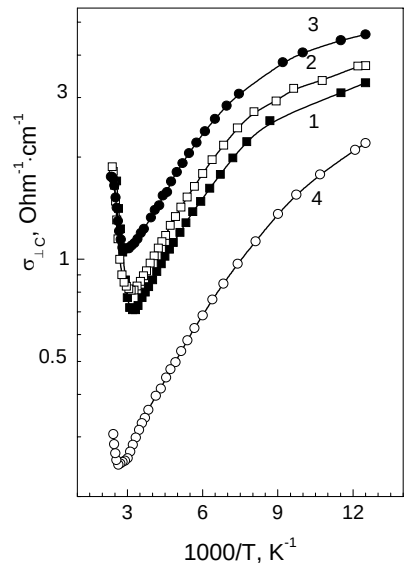

Fig. 2. Temperature dependences of the conductivity along the layers for samples from the fast (1 to 3) and slowly (4) cooled InSe ingots. The notation of curves 1-3 is the same as in Fig. 1.

© 2007, V. Lashkaryov Institute of Semiconductor Physics, National Academy of Sciences of Ukraine

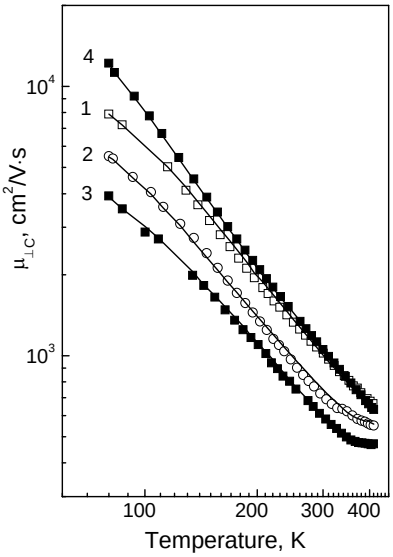

Fig. 3. Temperature dependences of the Hall mobility along the layers for samples from the fast (1 to 3) and slowly (4) cooled InSe ingots. The notation of curves 1 to 3 is the same as in Fig. 1. Symbols – the experimental data, lines – the calculated dependences: 1 to 3 – $\mu_{ph+BH+SC}$, 4 – μ_{ph+BH}.

Figure 3 shows the temperature dependence of the Hall electron mobility $\mu_{\perp C}$ along the layers for fast cooled samples 1 to 3 (curves 1-3). In comparison with the slowly cooled sample (curve 4), the influence of this technological procedure leads to its decrease and the appearance of some peculiarities in the high-temperature range. Like to the slowly cooled sample, there is no tendency to create a maximum in the $\mu_{\perp C}(T)$ dependences. That is, a transition to the predominant scattering of carriers by ionized impurities does not occur even at $T = 80$ K. In order to analyze the observed $\mu_{\perp C}(T)$ dependences, the contributions of various scattering mechanisms to the total mobility μ supposed to be expressed by the Matthiessen rule

$$\mu^{-1} = \sum_i \mu_i^{-1}$$

were determined as a result of numerical calculations for separate mechanisms μ_i. The temperature dependence of the mobility due to the lattice scattering has been analyzed on the basis of a three-dimensional model for the short-range interaction of electrons with homopolar optical phonons polarized along the crystallographic *C* axis [13, 14]. In this case, the drift mobility has the form

$$\mu_{ph} = \frac{4e}{3\sqrt{\pi} m^*} \int_0^\infty \tau(U) U^{3/2} \exp(-U) dU, \qquad (1)$$

where $U = \varepsilon / kT$, ε is the energy of carriers, k is the Boltzmann constant, τ is the relaxation time, and $m^* = \left(m_{\perp C}^2 \cdot m_{\| C}\right)^{1/3}$ is the average electron effective mass equal to 0.112 m_0 [11] for InSe. Like the majority of papers concerning the transport properties of InSe, our calculations were carried out for the low-energy phonon mode A_{1g}^1 ($\hbar\omega$ = 14.3 meV) which only deforms the In-In bonding at the electron-phonon coupling constant $g^2 = 0.051$.

Assuming the Brooks-Herring equation [15] to be true for the scattering by ionized impurities, the total mobility due to both mechanisms is given as $\mu^{-1} = \mu_{ph}^{-1} + \mu_{BH}^{-1}$. This expression well reproduces the $\mu_{\perp C}(T)$ dependence for the slowly cooled sample (curve 4 in Fig. 3), but it is not sufficient for the fast cooled samples. Let us analyze this situation by using sample 3 as an example (Fig. 4). If one determines the ion concentration N_i from the coincidence between the experimental $\mu_{\perp C}$ and calculated μ mobilities at 80 K, where the interaction with ions is most essential, the calculated curve goes over the experimental one at higher temperatures (curve 3 in Fig. 4). When the fitting is done at T = 293 K, the calculated $\mu(T)$ values are too low at the liquid nitrogen temperature (curve 1).

This circumstance along with the observed $\mu_{\perp C}(T)$ peculiarities at T > 300 K for the fast cooled samples lead to the necessity to take the additional scattering mechanism into account which should be stronger at high temperatures. As such a mechanism for *n*-InSe, the electron scattering by space-charge regions (SCRs) was considered in [16]. When the SCR radius R_{SC} is less than the carrier mean free-path, the regions act as scatterers. Assuming that free carriers cannot penetrate into such regions with effective cross-section Q and suggesting that it is related to the Debye screening length r_D as $Q \sim r_D^2$, we get the Weisberg expression for the corresponding mobility μ_{SC} [17] in the form

$$\mu_{SC} = \frac{4e^3 k^{3/2}}{\kappa \left(2m^*\right)^{1/2}} \frac{1}{N_{SC}} n T^{-3/2}. \qquad (2)$$

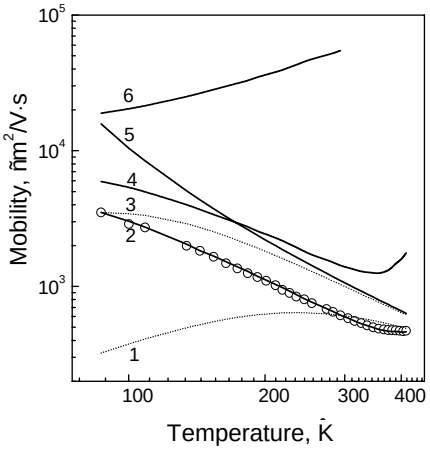

Fig. 4. Partial contributions of the different scattering mechanisms to the total mobility for sample 3 in Fig. 3. Symbols – the experimental data, lines – the calculated dependences: 1 and 3 – μ_{ph+BH}, 2 – $\mu_{ph+BH+SC}$, 4 – μ_{SC}, 5 – μ_{ph}, and 6 – μ_{BH}.

© 2007, V. Lashkaryov Institute of Semiconductor Physics, National Academy of Sciences of Ukraine

Table. Parameters of the *n*-InSe samples presented in Fig. 3.

Sample	80 K				
	n (cm^{-3})	$\mu_{\perp C}$ (cm^2/V·s)	Q (cm^2)	N_{SC} (cm^{-3})	N_i (cm^{-3})
1	2.51×10^{15}	7900	1.08×10^{-10}	1.70×10^{14}	7.37×10^{15}
2	4.15×10^{15}	5510	6.52×10^{-9}	3.22×10^{15}	6.52×10^{15}
3	7.50×10^{15}	3920	3.99×10^{-9}	9.93×10^{15}	9.91×10^{15}
4	1.15×10^{15}	12180	–	–	3.70×10^{15}

Here, κ is the InSe permittivity, and N_{SC} is the concentration of space-charge regions. The three above-mentioned scattering mechanisms give the total mobility

$$\mu^{-1} = \mu_{ph}^{-1} + \mu_{BH}^{-1} + \mu_{SC}^{-1} \ . \qquad (3)$$

From the fitting of the calculated curve based on Eq. (3) to the experimental data, we have obtained some parameters of scattering centers. They are listed in Table. For sample 3, the contribution of the different scattering mechanisms to the total mobility is shown in Fig. 4. As one can see from the obtained results, the peculiarities of the measured $\mu_{\perp C}(T)$ dependences above 300 K for the fast cooled samples are due to the interaction of electrons with SCRs. The abrupt increase of the free electron concentration due to the activation from the deep donor level leads to the increase of μ_{SC} with temperature, i.e. SCRs scatter less essentially because of their screening with electrons (curve 4 in Fig. 4).

The conductivity across the layers for InSe samples prepared from the same ingot parts is shown in Fig. 5. It makes possible to estimate the conductivity anisotropy. It is known [8, 10] that, in *n*-InSe, the ratio $\sigma_{\perp C}/\sigma_{||C}$ varies from several units up to 10^5. But the high anisotropy ratio cannot be supposed to be a result of a two-dimensional band structure, as the numerical calculations and many experimental data indicate the three-dimensional character of the bands forming the fundamental absorption edge. The wide variation of the anisotropy is due to the presence of uncontrolled impurities including aggregates of over-stoichiometric In or dopants at the interlayer stacking faults. Such a disordering restricts the electron transport along the *C* axis. Therefore, the obtained high values of $\sigma_{\perp C}/\sigma_{||C}$ (~10^3) for fast cooled samples 1 and 2 in Fig. 5 indicate the high amount of defect interlayer spaces. As for sample 3 from the upper part of the ingot, the suddenly low anisotropy ratio ($\sigma_{\perp C}/\sigma_{||C}$ is even below unity at 300 K) takes place most likely due to possible indium shorting jumpers between the layers what, in turn, results in the increase of $\sigma_{||C}$.

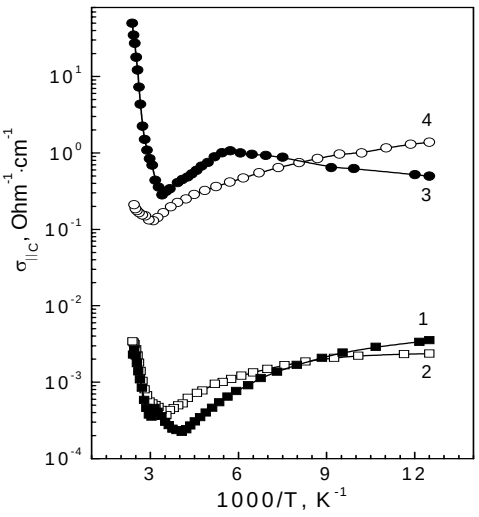

Fig. 5. Temperature dependences of the conductivity across the layers for samples from the fast (1 to 3) and slowly (4) cooled InSe ingots. The notation of curves 1 to 3 is the same as in Fig. 1.

4. Conclusions

Electrical characteristics of InSe single crystals grown by the Bridgman method essentially depend on cooling conditions of the ingots after ending the crystal growth. In comparison with the conventional cooling under conditions of a "switched-off" furnace, the fast cooling leads to an essential increase of the free electron concentration and a decrease of the Hall mobility along the layers and its peculiarities in the high-temperature range. For the samples from the fast cooled ingot, the interaction of electrons with space-charge regions becomes the effective scattering mechanism. The higher the temperature of the ingot parts before cooling, the higher the concentration of these regions.

Acknowledgement

This work was supported by the Science and Technology Center of Ukraine (grant No. 3237).

References

1. A. Segura, J.P. Guesdon, J.M. Besson, A. Chevy, Photoconductivity and photovoltaic effect in indium selenide // *J. Appl. Phys.* **54**(2), p. 876-888 (1983).
2. Z.D. Kovalyuk, V.M. Katerynchuk, I.V. Mintyanskii, A.I. Savchuk, O.M. Sydor, γ-Radiation influence on the photoelectrical properties of oxide – p-InSe heterostructure // *Mater. Sci. Eng. B* **118** (1), p. 147-149 (2005).
3. Z.D. Kovalyuk, V.M. Katerynchuk, T.V. Betsa, Photoresponse spectral investigations for anisotropic semiconductor InSe // *Optical materials*, **17** (2), p. 279-281 (2001).
4. M. Balkanski, Solid-state microbatteries for electronics in the 21st century // *Solar Energy Materials and Solar Cells* **62**(1-2), p. 21-35 (2000).

© 2007, V. Lashkaryov Institute of Semiconductor Physics, National Academy of Sciences of Ukraine

5. Yu.I. Zhirko, I.P. Zharkov, Z.D. Kovalyuk, M.M. Pyrlja, V.B. Boledzyuk, On Wannier exciton 2D localization in hydrogen intercalated InSe and GaSe layered semiconductor crystals // *Semiconductor Physics, Quantum Electronics & Optoelectronics* **7**(4), p. 404-410 (2004).
6. K. Imai, K. Susuki, T. Haga, Y. Hasegava, Y. Abe, Phase diagram of In – Se system and crystal growth of indium monoselenide // *J. Cryst. Growth* **54** (3), p. 501-506 (1981).
7. Y. Nishina, K. Kuroda, Lattice instability of IIIB – VIB layer compounds // *Physica B+C* **99**(1-4), p. 357-360 (1980).
8. P.I. Savitskii, I.V. Mintyanskii, Z.D. Kovalyuk, Annealing effect on conductivity anisotropy in indium selenide single crystals // *Phys. status solidi* (*a*) **155** (2), p. 451-460 (1996).
9. P.I. Savitskii, Z.D. Kovalyuk, I.V. Mintyanskii, Thermally stimulated changes in the defect structure of indium monoselenide // *Neorganich. Materialy* **33**(9), p. 897-901 (1997) (in Russian).
10. P.I. Savitskii, Z.D. Kovalyuk, I.V. Mintyanskii, Anisotropy of electrical conductivity in indium selenide // *Ibid.* **32**(4), p.361-365 (1996) (in Russian).
11. A. Segura, F. Pomer, A. Cantarero, W. Krause, A. Chevy, Electron scattering mechanism in n-type indium selenide // *Phys. Rev. B* **29**(10), p. 5708-5717 (1984).
12. A. Segura, K. Wünstel, A. Chevy, Investigation of impurity levels in n-type indium selenide by means of Hall effect and deep level transient spectroscopy // *Appl. Phys. A* **31** (2), p. 139-145 (1983).
13. R.C. Fivaz, Ph. Schmid, Transport properties of layered semiconductors, In: *Optical and Electrical Properties* / Ed. P.A. Lee. D. Reidel Publ. Co., Dordrecht, 1976, p. 343-384.
14. Ph. Schmid, Electron-lattice interaction in layered semiconductors // *Nuovo Cim. B* **21**(2), p. 258-272 (1974).
15. K. Seeger, *Semiconductor Physics*. Springer, Vienna, 1973.
16. P.I. Savitskii, Z.D. Kovalyuk, I.V. Mintyanskii, Space-charge region scattering in indium monoselenide // *Phys. status solidi* (*a*), **180**(2), p. 523-531 (2000).
17. L.R. Weisberg, Anomalous mobility effects in some semiconductors and insulators // *J. Appl. Phys.* **33**(5), p. 1817-1821 (1962).

© 2007, V. Lashkaryov Institute of Semiconductor Physics, National Academy of Sciences of Ukraine